IJFANS INTERNATIONAL JOURNAL OF FOOD AND NUTRITIONAL SCIENCES

ISSN PRINT 2319 1775 Online 2320 7876

 UGC CARE Listed (Group-1) Journal Volume 11 Iss 12, 2022

Development and Characterization of Transfersomes for Improved Transdermal Administration of Ketoprofen

Jitendra Singh Rajawat[a]*, R.P.S. Rathore[b].

[a]Bhupal Nobles' College of Pharmacy, Udaipur-313001, Rajasthan

[b]Bhupal Nobles' Institute of Pharmaceutical Science, Udaipur-313001, Rajasthan

*Corresponding author: Email: jeetupharma@gmail.com

Abstract: Examining transfersomes as a potential transdermal delivery mechanism for the poorly soluble medication was the objective of the current investigation. Ketoprofen, in order to get around the problems with taking it orally. The rotational vacuum evaporation and sonication process, along with a non-ionic surfactant (span 80) and phosphatidyl choline, were used to create several transfersomal formulations. The finished products were examined using a variety of techniques, including light microscopy, particle size analysis, turbidity, drug content, rheology, surface charge and density, penetration ability, in vitro release, ex vivo permeation, skin irritation/sensitivity study, and stability studies. We used the paw edema test paradigm to see whether the improved formulation had any anti-inflammatory effects on rats. The drug was found to be compatible with the excipients in FTIR and DSC investigations. Findings showed that all formulations effectively captured Ketoprofen with consistent drug content. Because it demonstrated the highest levels of drug entrapment (95.69±0.17%) and cumulative percent drug release (74.34±0.34), the optimal formulation (F4-S1-R4) was determined to be a transfersomal formulation consisting of 85% phosphatidyl choline of the medication and 15% span 80. We evaluated the ex vivo permeation profiles of the various transfersomal formulations with F4-S1-R4. The F4-S1-R1 transfersomal formulation outperformed the F4-S1-R2, F4-S1-R3, F4-S1-R4, and F4-S1-R5 in terms of cumulative drug permeation and flux, as well as lag time ($p<0.05$). From the perspective of its skin application, the transfersomal formulation F4-S1-R4, which had a lower flux, may be preferred over other formulations owing to its longer impact and greater viscosity. Better application and the absence of skin irritation were further contributing factors. As a result, the research proved that the transfersomal formulation is a viable substitute for the traditional Ketoprofen formulations that had improved transdermal penetration.Keywords: In vivo study, Ketoprofen, Permeation studies, Transdermal, Transfersomes

ISSN PRINT 2319 1775 Online 2320 7876

 UGC CARE Listed (Group-1) Journal Volume 11 Iss 12, 2022

Introduction

Ketoprofen is a nonsteroidal anti-inflammatory drug (NSAID) that has analgesic and antipyretic effects. It is used to alleviate pain associated with menstruation, bone surgery, osteoarthritis, rheumatoid arthritis, juvenile rheumatoid arthritis, ankylosing spondylitis, Reiter's syndrome, bursitis, tendinitis, gouty arthritis, dysmenorrheal, and other symptoms. Like other nonsteroidal anti-inflammatory drugs (NSAIDs), ketoprofen is believed to block prostaglandin formation as part of its pharmacologic effect. The suppression of cyclooxygenase-1 and cyclooxygenase-2 is thought to be responsible for its anti-inflammatory actions..[1,2,3]

When faced with the challenges of oral administration, transdermal distribution of ketoprofen proves to be the superior choice. Several benefits, such as improved bioavailability, reduced frequency of administration, improved patient compliance, rapid termination of drug input, avoidance of GI incompatibility, variable Gl absorption, and first-pass metabolism are offered by the transdermal route in addition to its convenience and safety. [4,5,6].

Among the many active chemicals that could benefit from transfersomes' adaptable delivery strategy is an increase in their stability. In non-occlusive settings, their (quasi) metastable nature renders the vesicle membrane extremely flexible; as a result, the vesicles are so pliable that they may be bent and twisted to fit into stratum corneum pores smaller than a tenth of their own diameter [6,7,8,9]. Therefore, particles as small as 200-300 nm can pass through unbroken skin. This is mainly because of the incredibly robust membrane flexibility that enables the transfersomal vesicles to enter a restricting pore after they have lodged in it. [9,10,11].

This study aims to improve the bioavailability of ketoprofen by incorporating it into the transfersomal system for transdermal administration, thus avoiding the issues associated with its oral delivery and increasing the drug's penetration through the skin.

Mechanism of Transport

To get past the stratum corneum's internal sealing lipids, transferosomes squeeze themselves through the skin. The current method for improving penetration is employing the process of water evaporation to create a "osmotic gradient" when the lipid suspension (transferosomes) is applied to the skin's surface. Due to this, concentration has no effect on the transit of these elastic vesicles. The vesicles are propelled to their destination by the trans-epidermal hydration. The stratum corneum pores can be squeezed by the elastic vesicles. Applying a transferosome vesicle to a non-

ISSN PRINT 2319 1775 Online 2320 7876

 UGC CARE Listed (Group-1) Journal Volume 11 Iss 12, 2022

occluded biological surface, like skin, causes it to migrate into the deeper strata, which are rich in water, to ensure that the surface is adequately hydrated. The lipid bilayer of the vesicle may diffuse with the cell membrane during intracellular drug transport, similar to how drugs are normally taken in during endocytosis. Advanced elasto-mechanics principles, material transport, and hydration/osmotic force all contribute to the intricate process. [11,12,13,14].

Materials and Methods

Materials

Ketoprofen was received as a gift sample from B.E.C. Chemicals Roha, Maharashtra, India. Span 80 and phosphatidyl choline were obtained from Loba Chemi Pvt. Ltd., Mumbai, India and Sigma-Alorich Chemie, GmbH, Steinheim, USA. All other chemicals used in this study were of analytical grade.

Formulation of Ketoprofen Transfersomes

Using the traditional rotary evaporation sonication approach, phospholipid, surfactant, and ketoprofen-containing transfersomes were prepared [15]. A tiny amount of ethanol was added to a clean, dry, round-bottom flask containing the phospholipids and surfactant in the ratio that was needed. Reducing the pressure and operating at 40°C, rotary evaporation was used to extract the organic solvent. Overnight, we used a vacuum to extract any remaining solvents. After the lipid film had been coated, it was hydrated with a 7% v/v ethanol solution, which is the medication, by spinning it at 60 rpm for 1 hour. The resultant vesicles were allowed to sit at room temperature for two hours so that they may enlarge and develop into big vesicles with multiple layers. The goal was to create smaller vesicles, thus they were sonicated in a bath for 10 minutes. [16, 17].

All of the drug-loaded vesicular formulations were examined for maximum entrapment efficiency and for the appearance of drug crystals over a period of 14 days using an optimal microscope.

Drug-Excipient Interaction Study

The FTIR spectrophotometer (Tensor-27, SN-0046, Type-121716, Bruker) was used to measure the concentration of the drug ketoprofen as well as a mixture of the drug (100 mg) and excipients (100 mg each of span 80 and phosphatidyl choline). Data were gathered across a spectral range of 450-4000 cm^{21} after the sample was pretreated with potassium bromide. Additionally, both the pure drug and the drug mixed with excipients had their ultraviolet (UV) spectra recorded.

ISSN PRINT 2319 1775 Online 2320 7876

 UGC CARE Listed (Group-1) Journal Volume 11 Iss 12, 2022

Differential Scanning Calorimetry (DSC)

A predetermined range of 0 to 100 degrees Celsius was used to measure the differential scanning calorimetry (DSC) thermograms of the drug ketoprofen and a mixture of ketoprofen, Span 80, and phosphatidylcholine. A solid metal pan was used to correctly weigh 2 mg of the sample, then it was sealed and crimped. The data were collected while the temperature was being raised by 10°C per minute and dry nitrogen was being expelled at a steady rate of 20 ml per minute.

X-Ray Diffrection Crystallography

Fluorescence Microscopy Scintaz X-ray powder diffractometry was used to conduct the crystallography of Pure Ketoprofen. The instrument has a solid state detector, a step size of 0.05 degrees, a scan rate of 3 degrees per minute, and a range of 0–20,000 cps for the print pattern.

FT-IR Spectroscopy

A comparison was made between the FT-IR spectra of the pure drug and the spectra of the drug sample that was obtained. The FTIR spectra of the pharmaceuticals in bulk were recorded by means of a Shimadzu spectrophotometer. The drug's FTIR spectra were recorded using the KBr pellet technique. Accurately weighing and mixing 1 mg of ketoprofen with 100 mg of KBr, or a ratio of 1:100, was done in a pestle motor. Transparent discs were subsequently created using a pellet press. The discs were thereafter subjected to analysis in an FTIR spectrophotometer after being placed in the spectroscopic device.

Characterization of Transfersomal Formulations

Entrapment efficiency

The centrifuge method was used to determine the percentage entrapment efficiency. With 10 milliliters of pH 6.8 phosphate buffer saline (PBS), 100 milligrams of the transfersomal formulation was weighed and mixed. Centrifuged at 10,000 rpm for 40 minutes, the resultant transfersomal dispersion was collected from Mumbai, India (REMI LJ 01). To find the amount of free medicine, the transparent portion, called the supernatant, was used. A UV spectrophotometer (Shimadzu-1700, Japan) was used to measure the drug concentration in the final solution at 260 nm.[18,19].

The percentage of drug encapsulation was calculated by the following equation:

Entrapment efficiency (%) = (Ct -Cf/Ct)100

Where Ct is the concentration of total drug and Cf concentration of unentrapped drug.

ISSN PRINT 2319 1775 Online 2320 7876

 UGC CARE Listed (Group-1) Journal Volume 11 Iss 12, 2022

Morphology and Structure of Transfersomes

Through the use of Transmission Electron Microscopy (TEM): (Hitachi H7500, Japan), the shape and composition of the drug-loaded transfersomes were ascertained. A small amount of water was added to the transfersomal preparations. After that, a single drop of the diluted suspension was dropped onto the porous film grid, which was then stained with a 1% aqueous phosphotungestic acid solution, and then watched as it dried.

Optical microscopy was also used to see vesicles that had not been sonicated (Leica digital microscope, Germany). After spreading a thin coating of transfersomes onto a slide and covering it with a cover slip, the specimen was examined under a microscope.[20,21].

Number of Vesicle per Cubic mm

Among the many process factors, this one is crucial for achieving optimal composition. The number of vesicles per cubic mm was measured by optical microscopy using a hemocytometer. Transferosome formulations that did not undergo sonication might be diluted three to five times using a 0.9% sodium chloride solution. Using the following formula, we were able to determine the number of transfersomes in 80 tiny squires.

Total no. of transfersomes per cubic mm = Total no. of transfersomes counted Xdilution factor × 4000/Total no. of squares counted

Vesicle size and size distribution

A stage eyepiece micrometer that was calibrated using a micrometer scale was utilized in optical microscopy in order to conduct an analysis of the size of the transfersome vesicles prior to the application of sonication. The measurement of the Polydispersity Index (PDI) was accomplished through the use of dynamic light scattering using the Zetasizer HSA 3000 (Malvern Instruments Ltd, UK). A sonication procedure was performed on each and every sample before the PDI was determined.[22,23].

Surface Charge and Charge Density

Surface charge and charge density of transferosomes can be determined using Zetasizer HSA 3000 (Malvern Instruments Ltd, UK).

Degree of Deformability Measurement or Permeability

The conduct of the deformability study is compared to the pure size using a combination of various microporous filters. The pore diameter of these filters ranges from 50 nm to 400 nm, depending

ISSN PRINT 2319 1775 Online 2320 7876

 UGC CARE Listed (Group-1) Journal Volume 11 Iss 12, 2022

on the initial transfersomes suspension. A dynamic light scattering (DLS) measurement is taken after every pass to record the particle size and size distribution.

The degree of deformability was calculated by using the following formula,

D= J* (rv/rp)2

Where D = deformability of vesicles membrane, J = amount of suspension which was extruded during 5 min, rv = size of vesicles (after passes), rp = pore size of the barrier.

Turbidity Measurements

An overall lipid content of 0.312 mm was achieved by diluting the transfersomes with distilled water. A UV-visible spectrophotometer (Shimadzu-1700, Japan) was used to detect the turbidity as the absorbance at 274 nm after a 5-minute quick mixing process using sonication. A nephelometer can be used to measure the turbidity of a medication in an aqueous solution..

Drug Content Determination

The amount of drug was determined by dissolving 100 mg of the formulation in 10 mL of ethanol. The mixture was analysed by a UV-Visible spectrophotometer at 274 nm against ethanol as a blank [24].

Viscosity Measurement and Rheological Behavior

Viscosity of the produced formulations was measured with spindle no. 4 (Brookfield DV-II+ pro viscometer) at 32.0 ± 0.1°C at various angular velocities [20]. The rheological behavior of the transfersomal gel formulations was assessed using a 40 mm cone with a 2.5 deg cone angle in a plate arrangement. At 25°C, rheology experiments were carried out in the shear rate range of 50.63–250.7 s^3. The consistency index and flow index were calculated from the Power law equation:

$\tau = Krn$

Taking log on both sides,

Where, τ = shear stress, r = shear rate, K = consistency index, n = flow index

Taking log on both sides,

$\text{Log } \tau = \text{Log } K + n \log r$

Thus from the plot of the log of shear stress versus the log of shear rate, the slope of the plot was taken as the flow index and the Y-intercept gave the consistency index.

ISSN PRINT 2319 1775 Online 2320 7876

 UGC CARE Listed (Group-1) Journal Volume 11 Iss 12, 2022

In Vitro Drug Release Studies Through Cellophane Membrane

The in vitro permeation behavior of ketoprofen from all transfersomal suspension formulations (including drug, phosphatidyl choline, and span 80) was studied using a cellophane membrane (Molecular weight cut of 12000-14000, HI Media Ltd, Mumbai, India). The Franz Diffusion cell's vertical type was created, manufactured, and verified before the permeation investigation. With a 2.303 cm^2 effective diffusion area, the cellophane membrane was positioned atop a diffusion cell assembly. A 22.5 mL phosphate buffer with a pH of 6.8 was used in the receptor compartment, which was kept at 37 ±0.5°C during the experiments while the receptor fluid was agitated at 100 rpm. On the donor compartment membrane, the produced formulation was applied. Every appropriate amount of time, an aliquot of 2 mL of sample was removed and quickly replaced with an equivalent volume of brand-new diffusion medium. A timeline was created by computing and plotting the total amount that seeped through the cellophane membrane. [25-28].

Release Kinetics

The release kinetics were examined by fitting data from in vitro permeation investigations into three different kinetic models: zero order, first order, and Higuchi's model. The data were fitted into the Korsmeyer-Peppas model as the log cumulative percentage of drug released vs. log time in order to ascertain the mechanism of drug release. The exponent n was then computed from the slope of the straight line. In the slab matrix, the diffusion mechanism is fickian if the exponent is 0.5; non-fickian if 0.5<n <1.0, n 1 to Case II (relaxational) transport, and super case II transport if n > 1..

Stability Studies

It is possible to define the stability of the product as the capacity of a certain formulation to continue to conform to the physical, chemical, therapeutic, and toxicological standards. The improved formulation F4-S1-R4 was kept in glass vials at room temperature for three months before being placed in a refrigerator at a temperature of four to eight degrees Celsius. A number of parameters, including morphology, drug leakage, and drug entrapment, were examined at certain time intervals, namely at 0, 15, 30, 45, 60, 75, and 90 days.

Statistical Analysis

The research was conducted in duplicate for each and every one of the trials. With the help of Student's unpaired t-test, the statistical analysis was carried out. The slope of the linear part of the

ISSN PRINT 2319 1775 Online 2320 7876

 UGC CARE Listed (Group-1) Journal Volume 11 Iss 12, 2022

cumulative amount penetrated vs time plot was obtained in order to calculate the steady-state flux. The linear component of the cumulative quantity penetrated versus time curve was extrapolated to the abscissa in order to calculate the lag time, which is an abbreviation for "lag time." The enhancement ratio of the flux (Epen) was calculated as:

Epen = Ptreatment/Pcontrol

Where Ptreatment is the flux of formulation and Pcontrol is the flux of the control group.

Results and Discussion

Optimization Effect of various non-ionic surfactants on entrapment efficiency

The entrapment efficiency of many transfersomal formulations containing various types of non-ionic surfactant (tween 20, tween 80, span 20, span 80, and brij 35) was measured in order to optimize the type of non-ionic surfactant in the transfersomal formulation. Table 1 shows that the entrapment efficiency of F1 to F5 ranged from 42.9% to 38.3%. For the span 80 (F4), the maximum entrapment efficiency achieved was 94.9%. The HLB value of the non-ionic surfactant in the bilayer determines the entrapment effectiveness in transfersomes. Table 1 made it evident that the formulation with span 80 (F4) had the highest entrapment effectiveness. The only likely explanation for this is that span 80 has a lower HLB value than other non-ionic surfactants included in the transfersomal formulation. In order to determine the maximal drug-loading efficiency for each solvent system, F4 was utilized.

Effect Of Various Solvents on Drug Entrapment Efficiency

The trapping efficiency of several transfersomal formulations with distinct solvent types (methanol, ethanol, and chloroform) was examined in order to optimize the kind of solvent in the formulation. F4-S1 to F4-S3 had an entrapment efficiency of 87.7% to 64.7%, according to Table 1. Methanol (F4-S1) had the highest entrapment efficiency of 89.7%. A higher entrapment efficiency is likely attributable to methanol's increased fluidity and intralamellar distance of vesicular membranes [25, 26]. Viscosity and intralamellar distance of the vesicular membrane determine the entrapment efficiency in transfersomes. The formulation comprising methanol (F4-S1) yielded the highest entrapment efficiency, as demonstrated by Table 1. For each lecithin to surfactant ratio (70:30, 75:25, 80:20, 85:15, 90:10), the highest drug-loading efficiency was thus determined using F4-S1.

ISSN PRINT 2319 1775 Online 2320 7876

 UGC CARE Listed (Group-1) Journal Volume 11 Iss 12, 2022

Effect of Phosphatidylcholine to Span 80ratio on drug entrapment efficiency

The trapping efficiency of several transfersomal formulations with distinct solvent types (methanol, ethanol, and chloroform) was examined in order to optimize the kind of solvent in the formulation. F4-S1 to F4-S3 had an entrapment efficiency of 87.7% to 64.7%, according to Table 1. Methanol (F4-S1) had the highest entrapment efficiency of 89.7%. A higher entrapment efficiency is likely attributable to methanol's increased fluidity and intralamellar distance of vesicular membranes [25, 26]. Viscosity and intralamellar distance of the vesicular membrane determine the entrapment efficiency in transfersomes. The formulation comprising methanol (F4-S1) yielded the highest entrapment efficiency, as demonstrated by Table 1. For each lecithin to surfactant ratio (70:30, 75:25, 80:20, 85:15, 90:10), the highest drug-loading efficiency was thus determined using F4-S1.

Table 1: Optimization of non-ionic surfactants (F1-F5), solvents (F4-S1-F4-S3) and Phosphatidylcholine to Span 80 ratio (F4-S1-R1-F4-S1-R5) for Transfersomal formulation of Ketoprofen

Formulations	Non-Ionic Surfactants	Solvent	Phosphatidyl Choline: Span 80 ratio	% Entrapment Efficiency
F1	Tween 20	Methanol	80:20	42.9 ± 0.12
F2	Tween 80	Methanol	80:20	44.2±0.14
F3	Span 20	Methanol	80:20	53.7±0.12
F4	Span 80	Methanol	80:20	94.9±0.32
F5	Brij 35	Methanol	80:20	38.3±0.25
F4-S1	Span 80	Methanol	80:20	89.7±0.22
F4-S2	Span 80	Ethanol	80:20	67.2±0.04
F4-S3	Span 80	Chloroform	80:20	64.7±0.31
F4-S1-R1	Span 80	Methanol	70:30	53.2±0.22
F4-S1-R2	Span 80	Methanol	75:25	67.9±0.04
F4-S1-R3	Span 80	Methanol	80:20	63.71±0.31
F4-S1-R4	Span 80	Methanol	85:15	95.69±0.17
F4-S1-R5	Span 80	Methanol	90:10	88.3±0.11

Data are represent of mean plus/minus S * D (n = 3) .

ISSN PRINT 2319 1775 Online 2320 7876

 UGC CARE Listed (Group-1) Journal Volume 11 Iss 12, 2022

Differential Scanning Calorimetry (DSC)

The DSC thermogram result (figure 1) shows that there is no shifting of the peak of Ketoprofen occurs when it is mixed with Span 80 and Phosphatidyle choline. So this mixture follows the protocol of drug-excipients compatibility.

X- Ray Diffraction Crystallography of Pure Ketoprofen

The result of X- Ray Diffraction crystallography of Pure Ketoprofen confirmed that drug is crystalline in nature and various peaks are depicted in figure 2.

Drug-Excipients Compatibility Study via Ft-Ir Spectroscopy

The typical IR absorption peaks of KF are shown in Figure 3 for both the pure medication Ketoprofen and the mixture of Ketoprofen, Span 80, and phosphatidylcholine. The peaks are located at 2978, 2938 cm -^ prime, 2876 cm -^ 1, 1693 cm-1, 1599 cm-¹, 1442 cm -^ 1, 1369 cm-1, and 825640 cm-1. The pure drug's formulation F3's FTIR spectra showed that the typical peaks of ketoprofen remained unchanged in terms of their placements. following effective encapsulation, suggesting that the medication and the polymers utilized did not interact chemically.

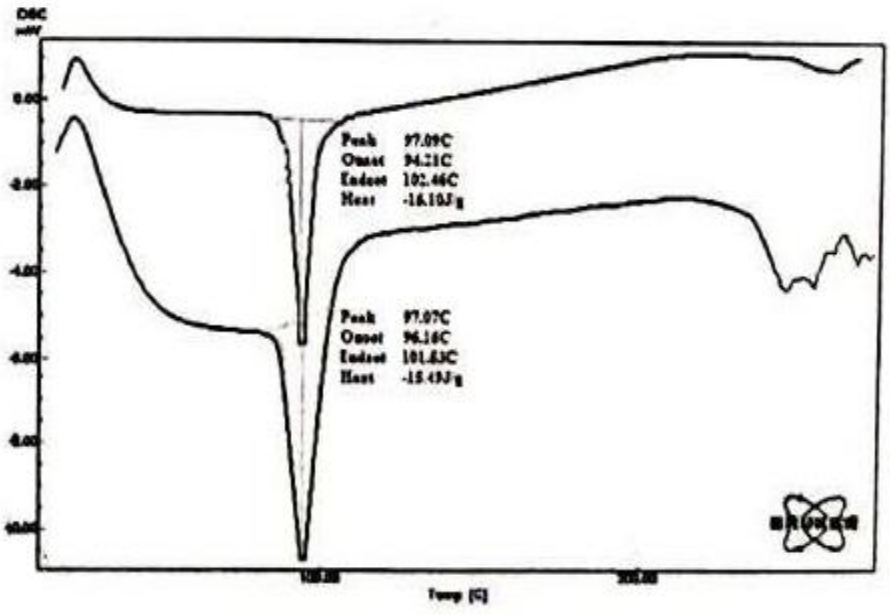

Figure 1: DSC of Pure Ketoprofen and mixture of Ketoprofen, Span 80 and Phosphatidylecholine

ISSN PRINT 2319 1775 Online 2320 7876

 UGC CARE Listed (Group-1) Journal Volume 11 Iss 12, 2022

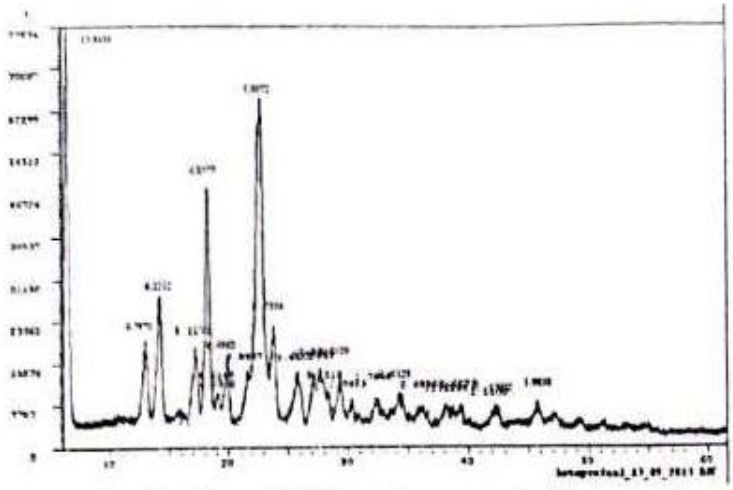

Figure 2: X-Ray Diffraction crystallography of Pure Ketoprofen

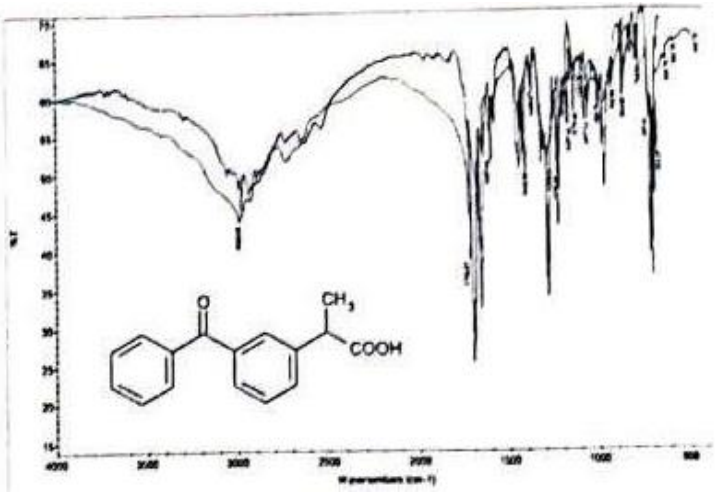

Figure 3: FTIR of pure Ketoprofen and mixture of Ketoprofen, Span 80 and Phosphatidyl choline

Table 2: Characteristic IR Absorption Peaks (Cm-¹) of Ketoprofen.

Characteristic IR Absorption Peaks (Cm-')	Groups
1697.38	C=O stretching ketones
1134.57, 1174.86, 1194.79, 1227.84, 1285.34	C=O stretching and bending
2978.67	O-H stretching carboxylic acid
1420	O-H bending carboxylic acid
1284.34, 1319.28	C-O stretching phenolics
1078.31, 1134.57, 1174.86, 1194.79, 1227.84, 1285.34.	C-H in plane bending - Aromatic
691.02, 703.53, 716.75, 773.10, 787.29	C-H out of plane bending-disubstituted
1445.31, 1420.60, 1598.20	C=C stretching aromatic

ISSN PRINT 2319 1775 Online 2320 7876

 UGC CARE Listed (Group-1) Journal Volume 11 Iss 12, 2022

Solubility

Ketoprofen's solubility was examined in the following solutions: 0.1N hydrochloric acid, water, methanol, phosphate buffer pH 4.6, phosphate buffer pH 6.8, and phosphate buffer pH 7.4. The solubility values were 0.001538 g/ml, 0.03651 g/ml, 0.00898 g/ml, 0.00718 g/ml, 0.01194 g/ml, and 0.01455 g/ml, respectively. It may be concluded from the results that Ketoprofen is sparingly soluble in methanol, phosphate buffer pH 6.8, and phosphate buffer pH 6.8. It is also somewhat soluble in water, 0.1N hydrochloric acid pH 1.2, and phosphate buffer pH 4.6. According to the pH dependent solubility, ketoprofen becomes more soluble at higher pH values.

Characterization of Transfersomes Formulations

Vesicle Shape

The vesicles seemed to be multilamellar, with their lamellae equally spaced around the core, according to optical inspection (Figure 4). No aggregation irregularities were found in the system. Confirming the vesicular properties, TEM results showed a positive picture with transfersomes appearing as spherical structures. (Figure 4).

Vesicle size and size distribution

Transfersome size characterisation is critical for effective and safe dosing. Vesicle size 32±0.27 nm was determined to be the lowest, as the surfactant content was kept to a minimum (Table 3). At a surfactant concentration of 20%, the vesicle size started to grow significantly, but it began to shrink beyond this point (Figure 4). Because micellar structure, rather than vesicles, formed, this resulted. The nano size range and low polydispersity index values were observed in all formulations. There was a narrow distribution and consistency of particle size within the formulation, as shown by the low polydispersity values (0.338-0.467) of the formulation (Figure 5). See figure 5 for the size disturbance of the F4-S1-R4 transfersome formulation.

ISSN PRINT 2319 1775 Online 2320 7876

 UGC CARE Listed (Group-1) Journal Volume 11 Iss 12, 2022

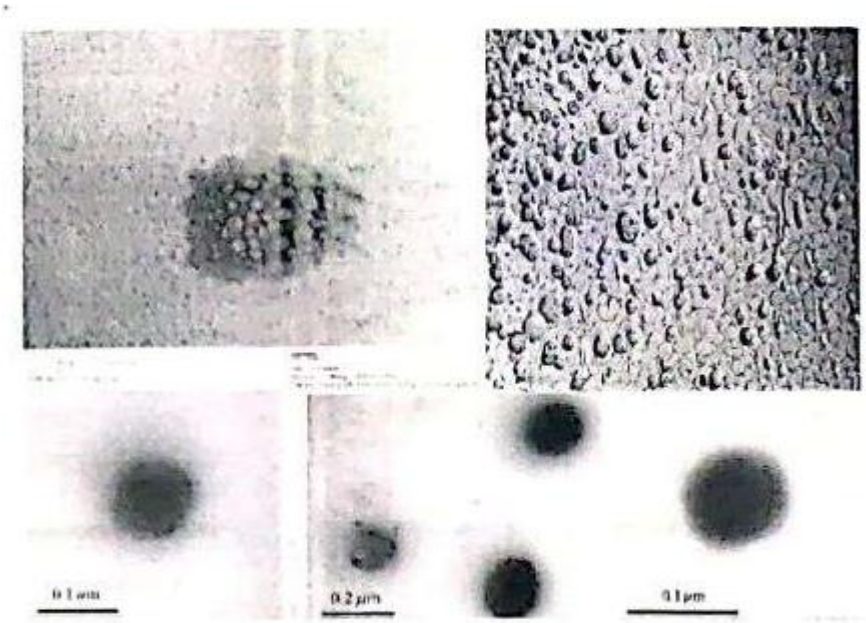

Figure 4: TEM photograph of Transfersomal formulations and of F4-S1-R4 formulation.

Degree of Deformability or Permeability Measurement

Transfersomes preparation is passed through a large number of pores of known size (figure 6). Particle size and size distributions are noted after each pass by dynamic light scattering (DLS) measurements and the size was found to be 57.1nm, 68.4nm, 70.7nm, 93.9nm 107nm (Figure 5)

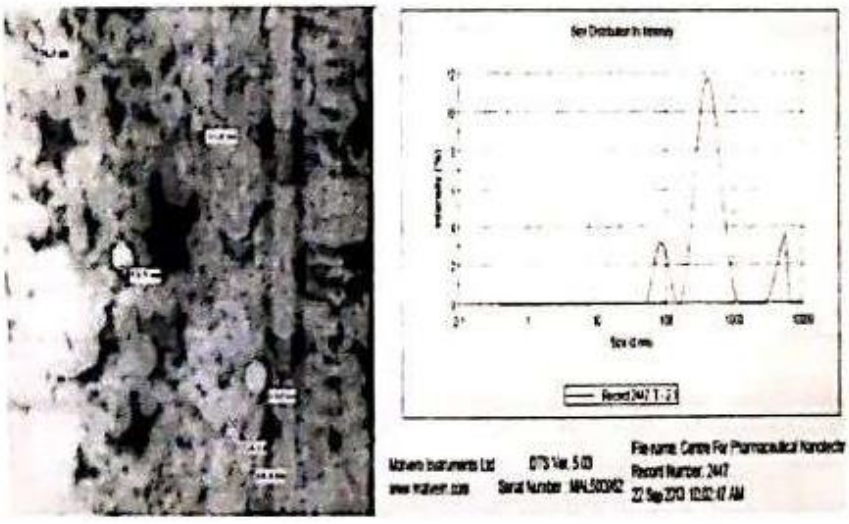

Figure 5: Particle size of different deformable transfersomal formulations and particle size distribution of F4-S1-R4.

ISSN PRINT 2319 1775 Online 2320 7876

 UGC CARE Listed (Group-1) Journal Volume 11 Iss 12, 2022

Number of Vesicles per Cubic mm

The number of vesicles per cubic mm counted by optical microscopy by using haemocytometer was found to be in the range from 32 ± 0.27 to 52 ± 0.21 (Table 3).

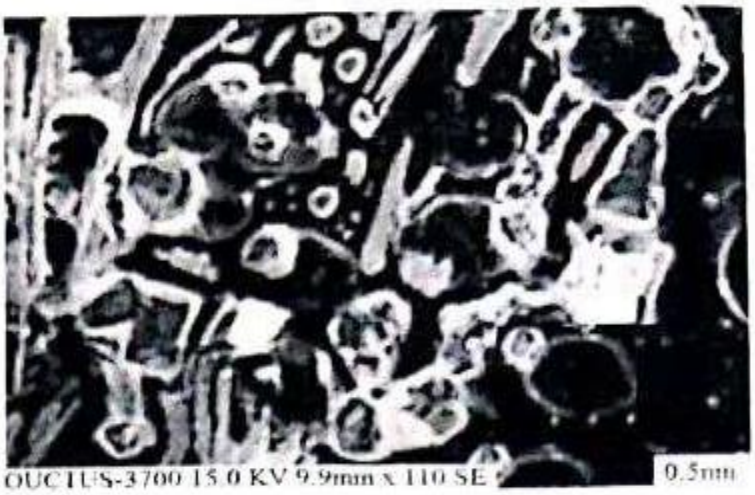

Figure 6: SEM photograph of Transfersomal F4-S1-R4 formulation.

Surface charge (Zeta Potential) and charge

density Surface charge(Zeta Potential) of transfersome formulations(F4-S1-R1 to F4-S1-R5) was in the range of -5.17mV to 12.42 mV (Table 3) is almost near to zero which shows neutral charge as the formulations consisted of nonionic surfactant components.

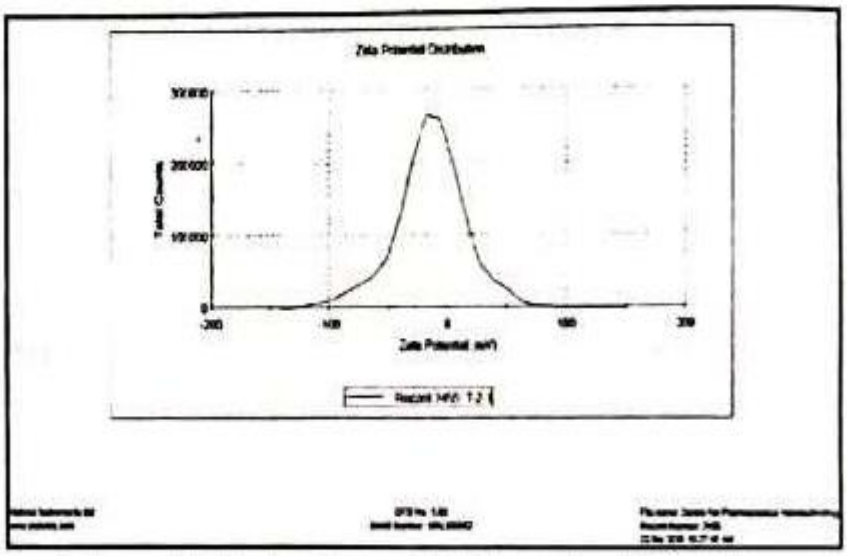

Figure 7: Zeta Potential Destribution of Transfersomal formulations

ISSN PRINT 2319 1775 Online 2320 7876

 UGC CARE Listed (Group-1) Journal Volume 11 Iss 12, 2022

Turbidity measurements

Transformation of transfersomes into mixed micelles is a concentration-dependent process and was governed mainly by the progressive formation of mixed micelles within the bilayer. To support the above fact, turbidity measurements were performed. The formulation F4-S1-R1 showed maximum turbidity i.e. 27.4±0.33 NTU. The results of the turbidity measurement studies (Table 3) sustained the fact that micelles were formed at higher concentrations of surfactant. Thus, it can be concluded that the turbidity of the deformable transfersomal formulations increased with an increase in surfactant concentration. After an optimum concentration, conversion of lipid vesicles into mixed micelles began, which have - negligible turbidity [29-32].

Drug content determination

The drug content among all of the batches was within the range from (97.4 plus/minus 0.34)% to 99.6 pm 0.21% (Table 3). The drug content of the developed formulations was not found to be significantly different ($p > 0.05$ t-test) from the added amount. The results indicate that the process employed to prepare the transfersomes was capable of producing formulations with consistent drug content [33-34].

Viscosity measurement and rheological behaviour

The viscosity± of the transfersomal formulation suspensions was found to be low (11.28±0.24 to 29.43±0.56 mPaS) and was not suitable for transdermal use, which justified the incorporation of the transfersomal suspension into a gel matrix, resulting in a transfersomal gel having a high value of viscosities. The viscosity of the transfersomal formulation suspension (F4-S1-R4) (29.43 plus/minus 0.56 mPaS) was significantly increased ($p < 0.05$. t-test) in case of the transfersomal gel (13726.33±1.87 mPaS) due to the incorporation of the carbopol 940 (1.0%) gel matrix, which made the formulation more suitable for the transdermal administration. The rheological behaviour of the gel formulation is governed by its components and the consistency of the formulation. The consistency index of the transfersomal gel formulation (F4-S1-R4) having high viscosity (13726.33±1.87) was found to be 82.859 Pa.S and had a flow index of (n) = 0.479 (Figure 8). The flow index n is a measure of the deviation of a system from Newtonian behaviour (n = 1) A value of $n < 1$ indicates pseudoplastic flow or shear thinning; $n > 1$ indicates dilatant or shear thickening flow. Flow index confers an idea of the flowability of the formulation from the container. The gel showed a flow index of 0.479, indicating pseudoplastic flow behaviour. This pseudoplasticity

ISSN PRINT 2319 1775 Online 2320 7876

 UGC CARE Listed (Group-1) Journal Volume 11 Iss 12, 2022

results from a colloidal network structure that aligns itself in the direction of shear, thereby decreasing the viscosity as the shear rate increases. The pseudoplastic flow performance justifies that the developed system will require some force to expel.

Table 3: Entrapment efficiency, Number of vesicles per mm^3, Polydispersity index (PDI), Drug Content and turbidity of Transfersomal formulation

Formulation Code	Entrapment efficiency (%)	No. of vesicles per m m 3 1000X	PDI	Drug content (%)	Turbidity (NTU)	Zeta potential (mV)
F4-S1-R1	53.2±2.12	35±2.34	0.442±0.04	97.4±0.34	27.4±1.33	-6.50
F4-S1-R2	67.9±1.14	39 ±1.23	0.392±0.05	26.9±1.32	98.5±0.23	-5.17
F4-S1-R3	83.7±1.43	45±1.32	26.1±1.23	0.376±0.02	98.7±0.32	-7.32
F4-S1-R4	95.69±1.15	52±2.21	0.338±0.08	25.9±1.12	99.6±0.21	-9.10
F4-S1-R5	88.3±2.32	32±1.27	0.467±0.1	97.9±0.27	24.2±1.17	-12.42

Data are represent of mean ± SD (n = 3).

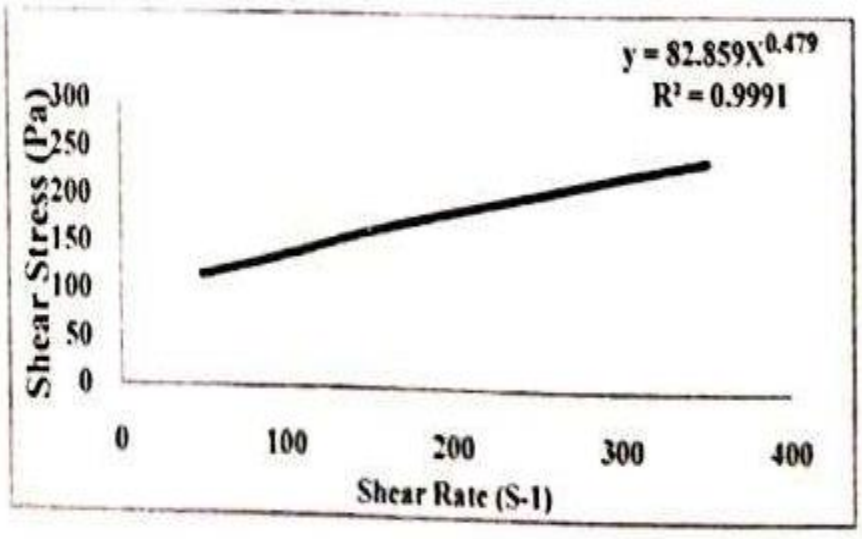

Figure 8: Rheogram of transfersomal gel formulation (F4-S1-R4).

In-vitro drug release studies through a cellophane membrane

In vitro drug release tests were conducted on each of the transfersomal formulations using a cellophane membrane. For every formulation, the total amount of drug release was determined. The results showed that out of all the transfersomal formulations tested, the F4-S1-R4 (with a 15%

ISSN PRINT 2319 1775 Online 2320 7876

Research Paper **© 2012 IJFANS. All Rights Reserved,** UGC CARE Listed (Group-1) Journal Volume 11 Iss 12, 2022

span 80) had the largest cumulative amount of drug release (74.34%) up to 24 hours, whereas the others ranged from 53.83% to 64.08%. In comparison to the other formulations, the rate of Ketoprofen release from F4-S1-R4 was noticeably higher ($P < 0.05$, t-test) (Figure 9, 10, 11, 12). Ketoprofen was shown to be released continuously from the transfersomal gel formulation, according to the release trials. F4-S1-R4 had the highest release due to its highly effective trapping and increased drug content. The optimal surfactant concentration of 15% also contributed to the maximum release from the vesicles; this was because the surfactant molecule formed stronger associations with the phospholipid bilayer at this concentration, leading to improved drug partitioning and, ultimately, higher drug release.

Table 4: Permeation kinetics of Ketoprofen transfersomal formulations

Formulation Code	Zero order model (r^2)	First order model (r^2)	Higuchi model (r^2)	Korsmeyer-peppas model (n)
F4-S1-R1	0.986	0.957	0.977	1.18
F4-S1-R2	0.990	0.907	0.991	1.19
F4-S1-R3	0.992	0.890	0.985	1.20
F4-S1-R4	0.991	0.910	0.994	1.21
F4-S1-R5	0.987	0.921	0.979	1.19

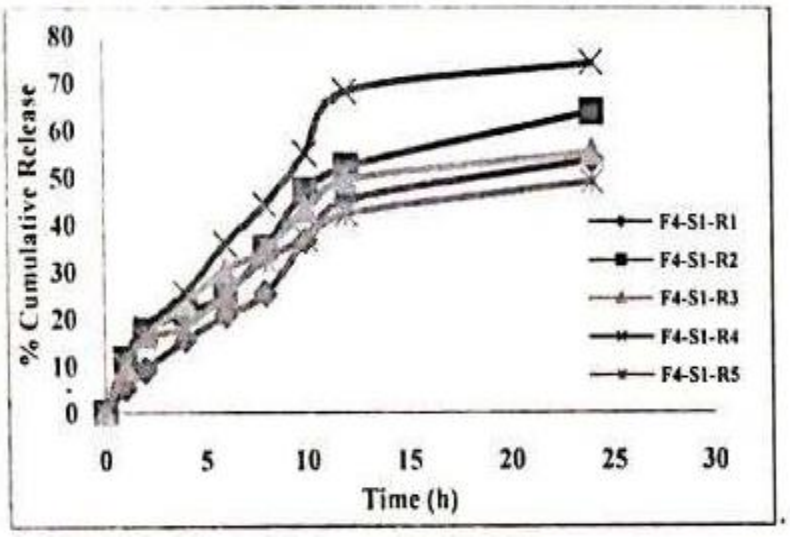

Figure 9: Zero order Release profile of Ketoprofen permeated across cellophane membrane from different transfersome formulations

ISSN PRINT 2319 1775 Online 2320 7876

 UGC CARE Listed (Group-1) Journal Volume 11 Iss 12, 2022

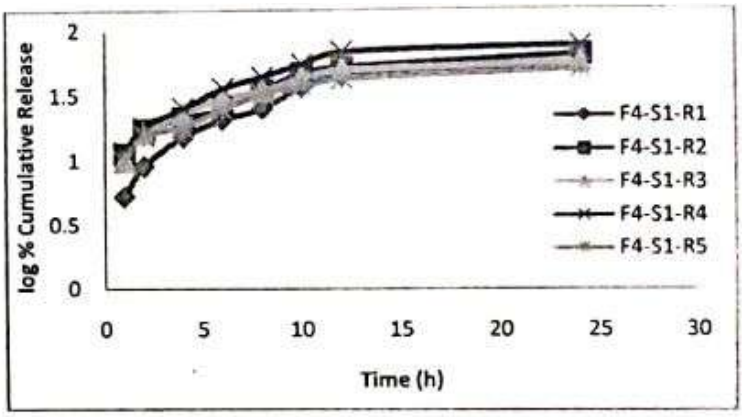

Figure 10: First order Release profile of Ketoprofen permeated across cellophane membrane from different transfersome formulations

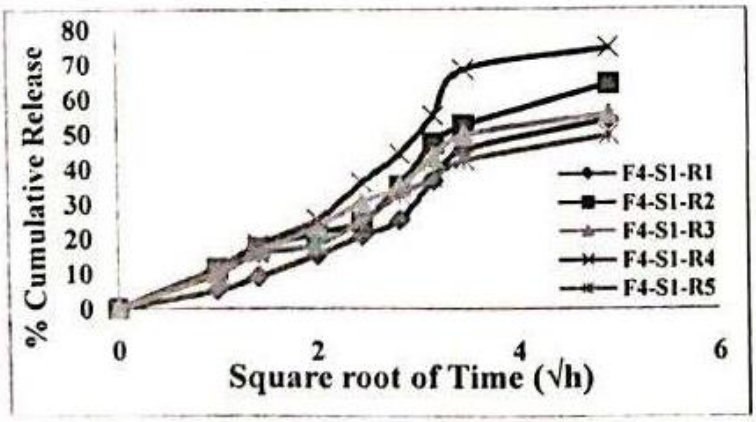

Figure 11: Higuchi profile of Ketoprofen permeated across cellophane membrane from different transfersome formulations

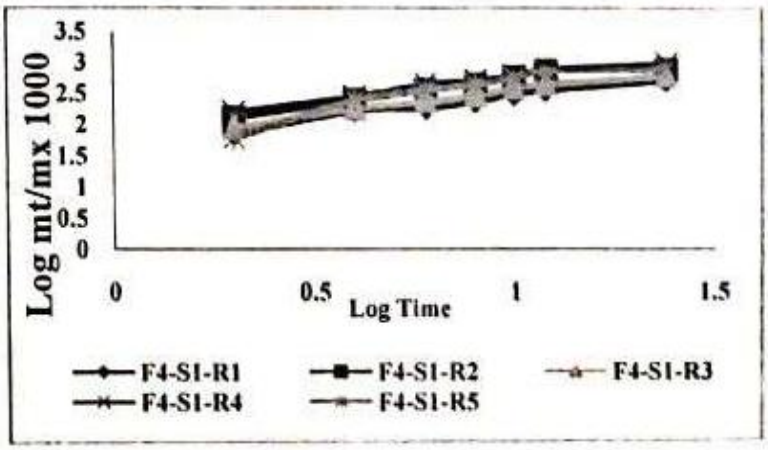

Figure 12: Korsemeyer pappas profile of Ketoprofen permeated across cellophane membrane from different transfersome formulations

ISSN PRINT 2319 1775 Online 2320 7876

 UGC CARE Listed (Group-1) Journal Volume 11 Iss 12, 2022

Interpretation of Release Mechanism

Based on the correlation coefficient values, the formulation F4-S1-R4 was shown to be the greatest fit for the Higuchi kinetic equation, surpassing both zero-order and first-order kinetics (Table 4 and Figure 9, 10). So, according to Higuchi's theory, the drug diffuses through the membrane, slowly but steadily penetrating it. Super case II was indicated by the best fitting obtained using the Korsmeyer-Peppas model with n > 1. It is well-established that case II transport happens when the chain relaxation process is noticeably slower than diffusion, further confirming that diffusion is the primary regulator of drug release. [35-37].

Stability Studies

The formulation that was optimized (F4-S1-R4) was seen in glass vials for a period of three months. During this time, it was visually observed at defined intervals under an optical microscope to look for changes in the consistency and appearance of the drug crystals. It was discovered that the consistency of the transfersomal formulations did not change after three months, and that there were no drug crystals that emerged even after three months, regardless of whether the formulations were stored at room temperature (35± 2 °C) or at a temperature of four degrees Celsius (plus or minus two degrees Celsius). It was also observed that the transfersomes were more stable when stored at refrigerator temperature. This was due to the fact that the formulation exhibited a higher entrapment efficiency (greater than 80%) and a higher percentage of drug retention (greater than 90%) than the formulation that was stored at room temperature, which demonstrated a low entrapment efficiency (greater than70%) and a higher percentage of drug retention (greater than 60%) at the end of three months (Figure 13).

ISSN PRINT 2319 1775 Online 2320 7876

 UGC CARE Listed (Group-1) Journal Volume 11 Iss 12, 2022

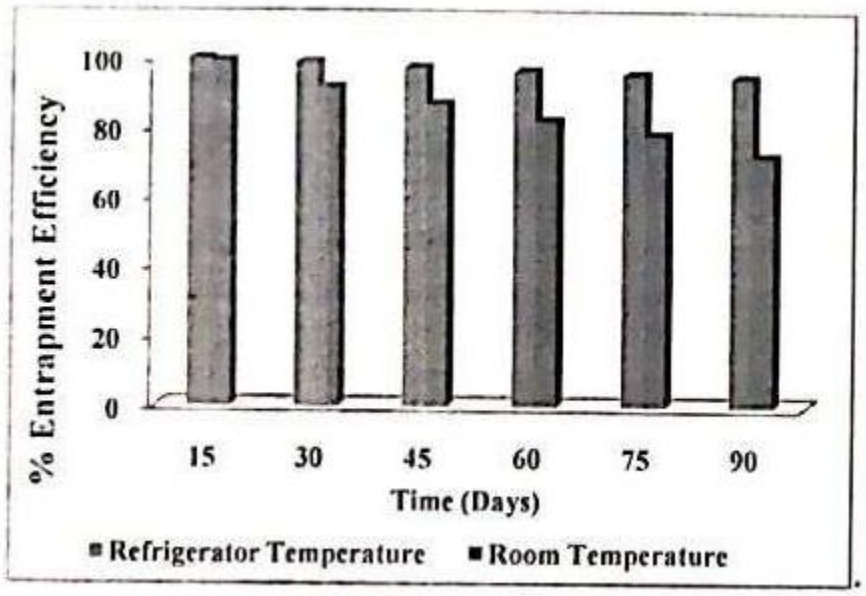

Figure 13: % Entrapment efficiency at refrigerator temperature and room temperature

Conclusion

According to the findings of the current research, the transfersomal formulation that involved the utilization of span 80 and phosphatidyl choline has the potential to be utilized for the purpose of enhancing the delivery of ketoprofen to the skin due to its exceptional release and permeation of the medication. While the mixture was being applied, there was no evidence of any skin irritation being noticed. The findings of these trials have been encouraging, and as a result, it is possible to administer ketoprofen using a formulation that is transferred to the skin through the transdermal route. It is therefore possible that the transdermal transfersomal formulation that was produced could prove to be a promising carrier for ketoprofen and other medications, particularly due to the fact that their production is straightforward and their scaling up is straightforward.

REFRENCES

1. Acharya, M.G. Ahmed, B.D. Rao, et al., Development and evaluation of ethosomal gel of lornoxicam for transdermal delivery: in-vitro and in-vivo evaluation, Manipal J. Pharmaceut. Sci. 2 (1) (2016) 14–20.
2. S. Gao, B. Tian, J. Han, et al., Enhanced transdermal delivery of lornoxicam by nanostructured lipid carrier gels modified with polyarginine peptide for treatment of carrageenan-induced rat

ISSN PRINT 2319 1775 Online 2320 7876

 UGC CARE Listed (Group-1) Journal Volume 11 Iss 12, 2022

paw edema, Int. J. Nanomed. 14 (2019) 6135–6150, https://doi.org/10.2147/IJN.S205295 PubMed PMID: 31447556; PubMed Central PMCID: PMCPMC6683961.

3. K. Pavani, M.K. Babu, Formulation and evaluation of Lornoxicam transferosomes as carriers for effective transdermal drug delivery, JIJoRiP, Biotechnology, Indian J. Res. Pharm. Biotechnol. 3 (6) (2015) 416.
4. N. Berger, A. Sachse, J. Bender, et al., Filter extrusion of liposomes using different devices: comparison of liposome size, encapsulation efficiency, and process characteristics, Int. J. Pharm. 223 (1–2) (2001) 55–68, https://doi.org/10.1016/s0378- 5173(01)00721-9.
5. A.A. Abdellatif, H.M. Tawfeek, Transfersomal nanoparticles for enhanced transdermal delivery of Clindamycin, AAPS PharmSciTech 17 (5) (2016 Oct) 1067–1074, https://doi.org/10.1208/s12249-015-0441-7 PubMed PMID: 26511937.
6. Blank IH, Scheuplein RJ. Permeability of the skin. Physiological Reviews. (1971) 51: 702-747.
7. Elias PM. Epidermal lipids: barrier functions and desquamation. Journal of Investigative Dermatology. (1983) 80: 445-495.
8. Williams ML, Elias PM. The extracellular matrix of stratum corneum Role of lipids in normal and pathological function. Criticla Review of Therapeutic Drug Carrier System (1987) 3:95-122.
9. Wertz PW. Lipids and barrier function of the skin. Acta Derm Venereol (2000) Supp 208: 7-11.
10. Jain N, Talegonkar S, Jain NK. New ways to enter the blood stream: Emerging strategies in transdermal drug delivery. The Pharma Review. (2004): 41-59.
11. Aulton EM. Pharmaceutics: The science of dosage forms design. Churchill Livingstone, Newyork, Harcourt publishers. 2nd edition. (2002): 499-33. Mm
12. Ansel HC, Loyd AV, Popovich NG. Pharmaceutical dosage system. Lippincott Williams and Willkins publication. 7th edition, 110-112.
13. Kumar P, Sankar C, Mishra B. Delivery of macromolecules through skin. The Indian Pharmacist. (2004): 7-17,

ISSN PRINT 2319 1775 Online 2320 7876

 UGC CARE Listed (Group-1) Journal Volume 11 Iss 12, 2022

14. Layek B, Mukherjee B. Tamoxifen citrate encapsulated sustained release liposomes: preparation and evaluation of physicochemical properties. Sci Pharm. (2010) 78: 507-515. http://dx.doi.org/10.3797/scipharm.0911-11
15. Maghraby EGMM, Williams AC, Barry BW. Skin delivery of 5-Fluorouracil from ultra deformable and traditional liposomes in vitro. J Pharm Pharmacol. (2001) 53: 1069-1076. http://dx.doi.org/10.1211/0022357011776450
16. Malakar J, Sen SO, Nayak AK, Sen KK. Formulation, optimization and evaluation of transferosomal gel for transdermal insulin delivery. Saudi Pharm J. (2012) 20: 355-363.
17. Guo J, Ping Q, Sun G, Jiao C. Lecithin vesicular carriers for transdermal delivery of cyclosporine A. Int J Pharm. (2000) 194: 201- 207.
18. Patel MR, Patel RB, Parikh JR, Solanki AB, Patel BG. Effect of formulation components on the in vitro permeation of microemulsion drug delivery system of fluconazole. AAPS PharmSciTech. (2009) 10: 917-923.
19. Gupta A, Prajapati SK, Balamurugan M, Singh M, Bhatia D. Design and development of a proniosomal transdermal drug delivery system for Captopril. Trop J Pharma Res., (2007) 6: 687-693.
20. Bachhav YG, Patravale VB. Microemulsion- based vaginal gel of Ketoprofen: Formulation, in vitro evaluation, and stability studies. AAPS Pharm Sci Tech. (2009) 10: 476-481.
21. Ah YC, Choi JK, Choi YK, Ki HM, Bae JH, A novel transdermal patch incorporating meloxicam: in vitro and in vivo characterization. International Journal of Pharmaceutics. (2010) 385: 12-19.
22. Ammar HO, Ghorab M. El-Nahhas SA. Higazy IM. Proniosomes as a carrier system for transdermal delivery of tenoxicam. Int J Pharm. (2011) 405: 142-152.
23. Bhowmik M, Sanchita D. Chattopadhyay D. Ghosh LK. Study of thermo-sensitive in-situ gels for ocular delivery. Sci Pharm. (2011) 79: 351-358.
24. Gupta A, Aggarwal G. Singla S, Arora R. Transfersomes: a novel vesicular carrier for enhanced transdermal delivery of sertraline: development, characterization, and performance evaluation. Scientia Pharmaceutica. (2012) 80: 1061-1080

ISSN PRINT 2319 1775 Online 2320 7876

 UGC CARE Listed (Group-1) Journal Volume 11 Iss 12, 2022

25. Kanno K, Wu MK, Agate DA, Fanelli BK, Wagle N, Scapa EF, Ukomadu C, Cohen DE. Interacting proteins dictate function of the minimal START domain phosphatidylcholine transfer protein/StarD2. . J. Biol. Chem. (2007) 282 (42): 30728-36.
26. Jain S, Jain N, Bhadra D, Tiwary AK, Jain NK. Transdermal delivery of an analgesic agent using elastic liposomes: Preparation, characterization and performance evaluation. Current Drug Delivery. (2005) 2: 222-233. http://dx.doi.org/10.2174/1567201054368020
27. Lichtenberg D, Robson RJ, Dennis EA. Solublization of phospholipids by detergents: structural and kinetic aspects. Biochim Biophys Acta. (1983) 737: 285-304. http://dx.doi.org/10.1016/0304- 4157(83)90004-7
28. F. Habib, M. Abdel Azeem, G. Fetih, et al., Mucoadhesive buccal patches of lornoxicam: development and in-vitro characterization, Bull. Pharm. Sci. Assiut Univ. 33 (2010) 59–68.
29. D. Ma, A.M. Green, G.G. Willsey, et al., Effects of acoustic streaming from moderateintensity pulsed ultrasound for enhancing biofilm mitigation effectiveness of drugloaded liposomes, J. Acoust. Soc. Am. 138 (2) (2015 Aug) 1043–1051, https://doi. org/10.1121/1.4927413 PubMed PMID: 26328720.
30. S. Madan, C. Nehate, T.K. Barman, et al., Design, preparation, and evaluation of liposomal gel formulations for treatment of acne: in vitro and in vivo studies, Drug Dev. Ind. Pharm. (2018 Nov 16) 1–10, https://doi.org/10.1080/03639045.2018. 1546310 PubMed PMID: 30442066.
31. T.M. Ibrahim, M.H. Abdallah, N.A. El-Megrab, et al., Transdermal ethosomal gel nanocarriers; a promising strategy for enhancement of anti-hypertensive effect of carvedilol, J. Liposome Res. 23 (2018 Nov) 1–14, https://doi.org/10.1080/ 08982104.2018.1529793 PubMed PMID: 30272506.
32. P. Negi, M. Aggarwal, G. Sharma, et al., Niosome-based hydrogel of resveratrol for topical applications: an effective therapy for pain related disorder(s), Biomed. Pharmacother. 88 (2017 Apr) 480–487, https://doi.org/10.1016/j.biopha.2017.01. 083 PubMed PMID: 28126673.
33. W.S. Zheng, X.Q. Fang, L.L. Wang, et al., Preparation and quality assessment of itraconazole transfersomes, Int. J. Pharm. 436 (1–2) (2012 Oct 15) 291–298, https://doi.org/10.1016/j.ijpharm.2012.07.003 PubMed PMID: 22796030.

ISSN PRINT 2319 1775 Online 2320 7876

34. A. Ahad, M. Aqil, K. Kohli, et al., Enhanced transdermal delivery of an anti-hypertensive agent via nanoethosomes: statistical optimization, characterization and pharmacokinetic assessment, Int. J. Pharm. 443 (1–2) (2013 Feb 25) 26–38, https://doi.org/10.1016/j.ijpharm.2013.01.011 PubMed PMID: 23313344.
35. I. Scognamiglio, D. De Stefano, V. Campani, et al., Nanocarriers for topical administration of resveratrol: a comparative study, Int. J. Pharm. 440 (2) (2013 Jan 20) 179–187, https://doi.org/10.1016/j.ijpharm.2012.08.009 PubMed PMID: 22909994.
36. K. Li, S. Gao, B. Tian, et al., Formulation optimization and in-vitro and in-vivo evaluation of lornoxicam ethosomal gels with penetration enhancers, Curr. Drug Deliv. 15 (3) (2018) 424–435, https://doi.org/10.2174/ 1567201815666171207163010 PubMed PMID: 29219057.
37. D. Kumbhar, P. Wavikar, P. Vavia, Niosomal gel of lornoxicam for topical delivery: in vitro assessment and pharmacodynamic activity, AAPS PharmSciTech 14 (3) (2013 Sep) 1072–1082, https://doi.org/10.1208/s12249-013-9986-5 PubMed PMID: 23818079; PubMed Central PMCID: PMCPMC3755149.